Proc. NIPR Symp. Upper Atmos. Phys., **12**, 73–85, 1998

PLASMA AND MAGNETIC FIELD IMPULSIVE VARIATIONS IN THE DUSKSIDE LLBL: A GEOTAIL OBSERVATION

Motoharu NOWADA[1,2], Tohru SAKURAI[1], Yutaka TONEGAWA[1] and Toshifumi MUKAI[2]

[1] *Tokai University, 1117, Kitakaname, Hiratsuka 259-1292*
[2] *Institute of Space and Astronautical Science, Sagamihara 229-8510*

Abstract: We examined impulsive variations in the magnetic field and the plasma moment data observed by the GEOTAIL spacecraft on November 30, 1994, when the spacecraft passed inside of the inner-boundary of the dusk side magnetopause. The impulses occurred successively within 30 min from 0510 to 0540 UT. The examination was mainly focused on the plasma characteristics revealed by the ion distribution function in the impulses, from which we found that there is a characteristic showing a coexistence of low energy and dense sheath-like ions and their accelerated ions. Thus, the impulse is revealed to be a signature showing the impulsive penetration of the sheath-like ions into the inner magnetosphere, and on the way a sudden acceleration for the penetrated ions to the intermediate energy between the magnetosheath ions and magnetospheric ions.

1. Introduction

Impulsive magnetic field variations were observed near the magnetopause by the ISEE-2 and -3 satellites. These interesting and peculiar variations have been studied by several researchers (RUSSELL and ELPHIC, 1978; PASCHMANN *et al.*, 1982; GOSLING *et al.*, 1990a, b; ELPHIC, 1995). Their characteristics are shown with a bi-polar signature of the magnetic field and associated low energy-dense sheath-like plasma. They are called the Flux Transfer Events (FTEs). From their studies, the present paradigm for interpreting FTEs was established, namely, that FTEs are tubes of interconnected magnetospheric and solar wind magnetic flux, in other words, transient and small-scale reconnection.

THOMSEN *et al.* (1987) demonstrated the characteristics of plasma distribution within FTEs using ion and electron velocity distribution functions and confirmed that FTEs contain a mixture of magnetosheath and magnetospheric plasmas. But there are no strong interactions between them, since the plasma distributions are consistent with a simple superimposition of the two interpenetrating plasmas. Impulsive variations of the plasma were also observed by the ISEE-1 satellite near the northern dawnside magnetopause (SCKOPKE *et al.*, 1981; SCKOPKE, 1991). They explained that the impulsive variations of the plasma number density and temperature were due to the intermittent tailward motions of the boundary layer with a large modulation of thickness and vortex flow motion. Impulsive variations of the magnetic field and plasma were also observed when GEOTAIL passed through the low latitude boundary layers (LLBL).

In this report, our attention is focused on the plasma property observed in association with these impulses and how the distribution function changed in the successive impulses. In order to examine the properties of the plasma, the dynamic spectrum of the energy (*E-t* diagrams) and its distribution function were simultaneously used.

The general information on the interesting impulse events observed on November 30 is introduced in Section 2. In Section 3 the detailed examinations of the ion distribution function including the *E-t* diagram are described. Summary and discussion are presented in the last section.

2. The Event of November 30, 1994

The GEOTAIL satellite observed the impulsive variations in the magnetic field and plasma moment on November 30, 1994, when the satellite was located on the postnoon side of the LLBL, as shown in Fig. 1. The satellite position is indicated with a black circle on the trajectory. The location was more inner boundary of the LLBL.

Figure 2 shows a summary plot of the magnetic field data including the low energy plasma observed by GEOTAIL for one hour period from 0500 UT to 0600 UT, when the satellite observed impulses successively. From top to bottom panels three components of the magnetic field, B_x, B_y, B_z, and its magnitude, B_t, plasma flow velocity, V_x, V_y, V_z, and its magnitude, V_t, and plasma number density, N (/cc), plasma temperatures, T_{yy} and T_{zz}, thermal pressure, magnetic pressure, total pressure and beta ratio, respectively. The region where the impulsive variation was observed is indicated with two black broken vertical lines.

A sudden decrease in the plasma temperature was observed at 0510 UT in association with a gradual increase of the magnetic field strength. This increase in the magnetic field accompanying sudden changes of the magnetic field orientation in both B_x and B_y components suggests that the magnetic field lines bent outward and the diamagnetic effect was caused by the development of field-aligned currents. Enhanced plasma density and simultaneous decrease in the plasma energy were observed in association with these magnetic impulses. These signatures mean that the sheath-like low energy ions suddenly penetrated into the inner magnetosphere.

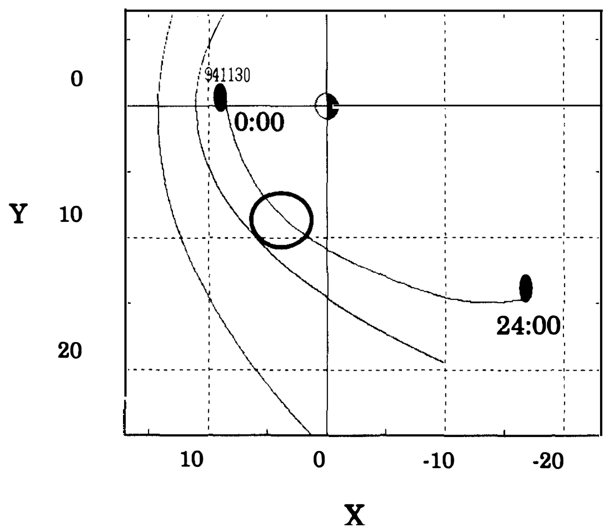

Fig. 1. The GEOTAIL trajectory on November 30, 1994 projected onto X-Y plane of SM coordinates. The black circle shows the GEOTAIL location during the period of one-hour from 0500 UT to 0600 UT.

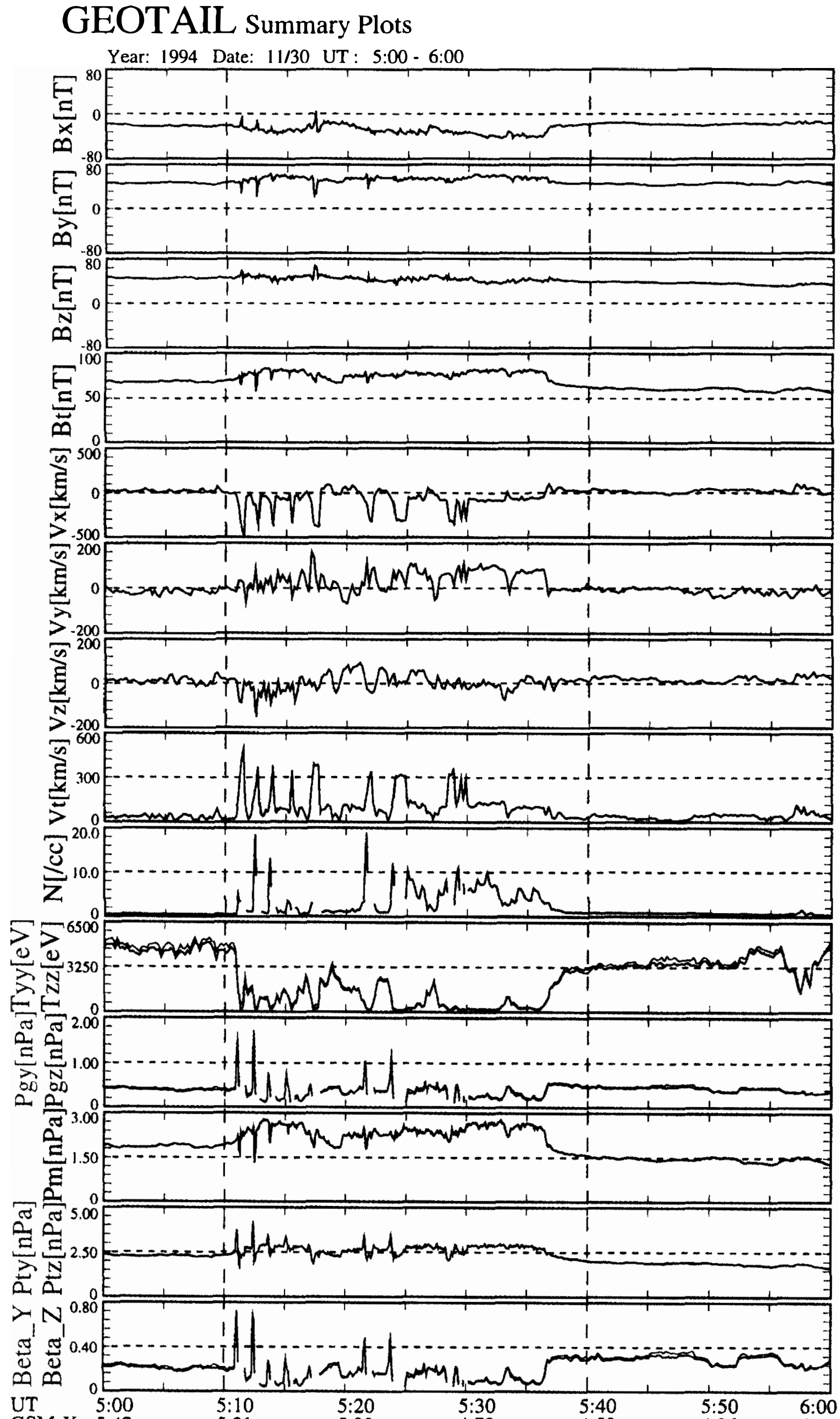

Fig. 2. A summary plot during one hour from 0500 to 0600 UT. From top to bottom panels show three components of the magnetic field, total magnetic field, three components of the plasma flow velocity, magnitude of the flow velocity, plasma number density, plasma temperature T_{yy} (perpendicular to the satellite spin axis) and T_{zz} (parallel to the satellite spin axis), gas pressure (nkT), magnetic pressure ($B^2/2\mu_0$), total pressure ($nkT+B^2/2\mu_0$) and Beta ratio ($nkT/B^2/2\mu_0$). The interval of 30 min from 0510 to 0540 UT indicated with the black dashed lines is the period when the impulses were observed.

This is also clearly recognized from the beta ratios ($\beta = nkT/B^2/2\mu_0$) at the moment as shown in the bottom panel of Fig. 2, where we recognize the increase in the plasma gas pressure in each impulse, although the background magnetic pressure was superior to the plasma pressure over the entire interval of our interest until 0538 UT. This background condition for both the plasma and magnetic field means that the satellite was located in the inner magnetosphere.

It must be noted here that these impulses are also associated with the impulsive high speed tailward plasma flow, which attained to about 500 km/s, implying that the tailward flowing solar wind plasma was observed by the satellite associated with the impulses even in the inner magnetosphere. However, this fact seems to be very important, and suggests that the magnetic field line of the magnetosphere was open to the solar wind at these moments and the solar wind plasma was observed by the satellite in the inner magnetosphere. If this is true, we would expect that the observed plasma consisted of the solar wind plasma alone with the impulses.

3. Distribution Function Characteristics of the Ions Observed during the Impulses

In this section we examine some essential characteristics of the ion velocity distribution functions observed in association with these impulses.

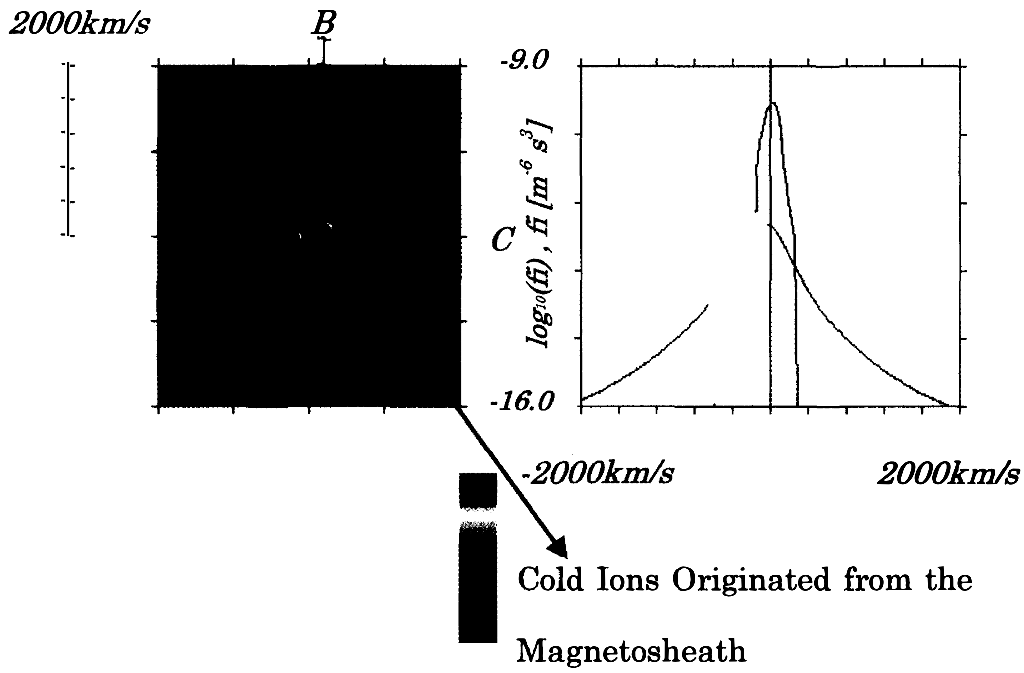

Fig. 3. Left panel: The ion phase space density in the plane including the axes of the parallel to the magnetic field line (B-axis) and the perpendicular ion flow direction (C-axis). Right panel: one dimensional ion distribution function cut along the magnetic field line (red dashed line). The typical phase space density of the magnetosheath ions under the quiet magnetic condition, which is characterized with the small velocity shown with the red color. On the other hand, one-dimensional distribution function is characterized with the monochromatic energy component.

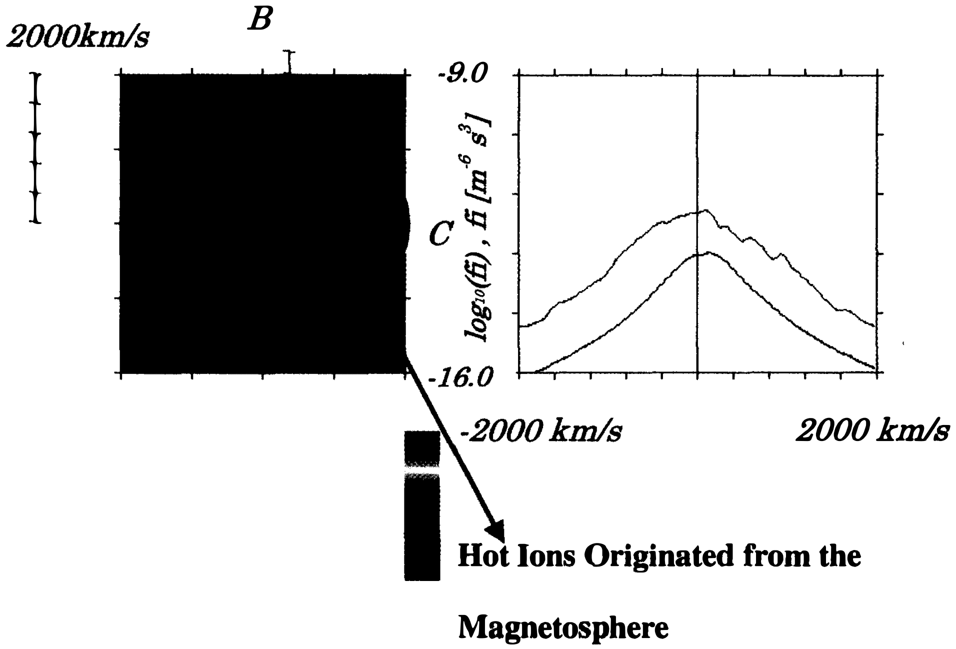

Fig. 4. Format is the same as in Fig. 3. Left panel: typical phase space density of the magnetospheric ions. Right panel: one dimensional distribution function under the normal condition. One-dimensional distribution is characterized with a plateau-like shape.

Before examining details of the distribution function, it is instructive to learn a typical velocity distribution function of ions observed both in the magnetosheath and magnetosphere.

Figures 3 and 4 show, respectively, such a typical ion distribution function obtained in each region by GEOTAIL on January 10, 1997, which was examined and reported by NAKAMURA *et al.* (1997). The left panel shows the ion phase space density profile projected onto the plane including the magnetic field and perpendicular ion flow vectors (the BC plane). The vertical and horizontal axes point to the direction of the magnetic field line (B-axis) and the perpendicular ion flow direction (C-axis), respectively. The upward direction of B-axis on the phase space density profile indicates the direction parallel to the magnetic field line. The right panel shows one dimensional distribution function deduced from the phase space density cut along the B-axis (red broken line).

From the left panel in Fig. 3, it is clearly understood that the ions of the magnetosheath are concentrated to the center, suggesting that energy of the magnetosheath ions is very low. On the other hand, the distribution of ions of the magnetosphere shown in Fig. 4 is circular and extends to high velocity, meaning that ions of the magnetosphere are hotter than those in the magnetosheath.

One dimensional distribution function presented in the right panel in each figure shows the distribution to be different; *i.e.*, a monotonic peak at the center in the distribution for the magnetosheath ions and a broad distribution extending to a high velocity for the magnetospheric ions.

By keeping these characteristics in our mind, we will examine the ion velocity distribution functions in the impulses observed on November 30, 1994. The upper three panels of Fig. 5 show the time variations of the ion density (top), the ion temperature

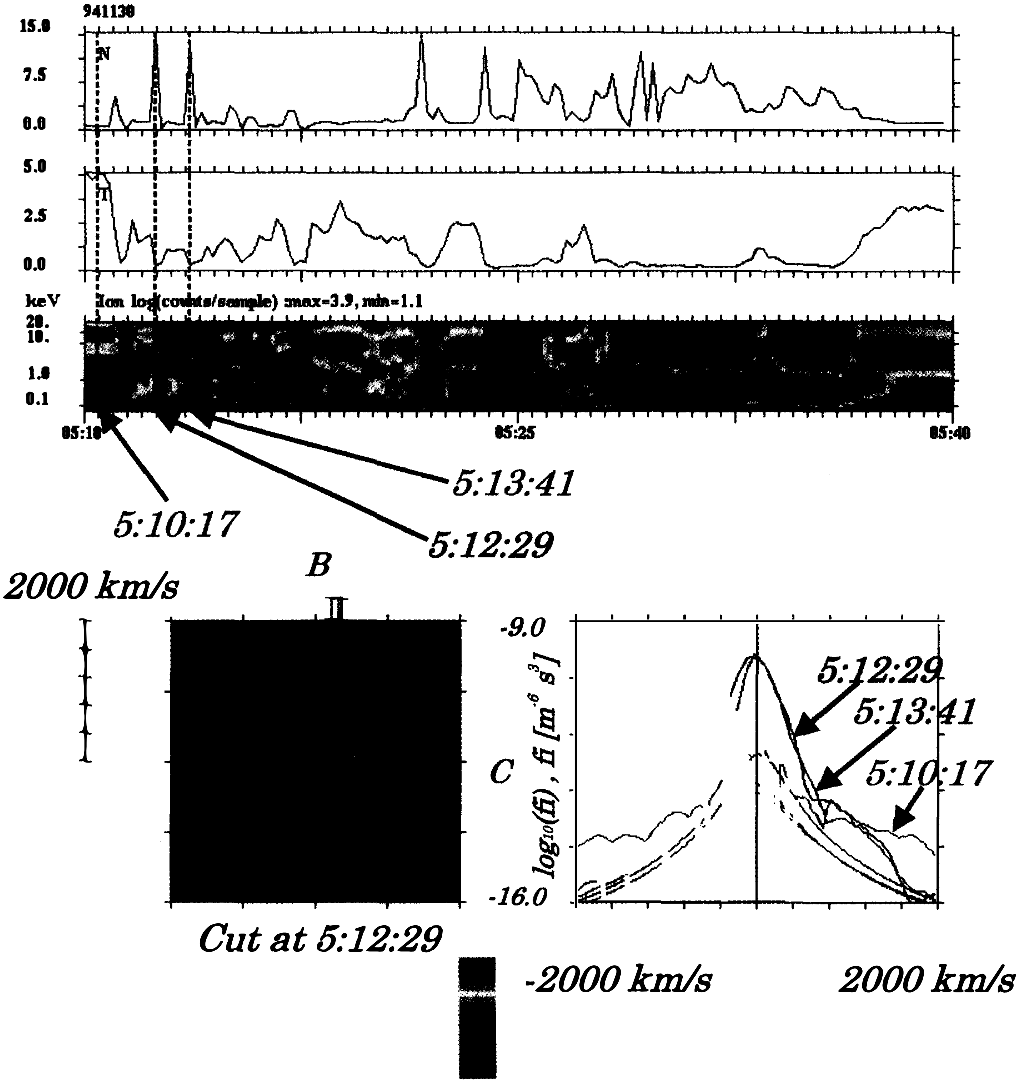

Fig. 5. From top to bottom panels show the ion number density, temperature, E-t diagram, the two dimensional ion distribution function (left panel) and the one dimensional ion distribution function (right panel). The two dimensional ion distribution function of the impulse observed at 0512:29 UT shows the extension of the distribution function in perpendicular direction to the magnetic field line. But a part of the contour of the accelerated ions originated from the magnetosheath characterized with the blue-green color is distributed to the field-aligned direction. One dimensional ion distribution function shows a coexistence of the sheath-like cold ions and their accelerated ions.

(middle) and *E-t* diagram (bottom), respectively. The lower left panel shows the ion phase space density profile for the second impulse occurred at 0512:29 UT marked with a red vertical broken line. Its one dimensional distribution function cut along the magnetic field line is displayed in the right panel with colored curves, in which two more profiles taken at the times of 0510:17 UT and 0513:41 UT are superimposed.

The phase space density shown in the left panel indicates that it consists of five portions of the ions colored with red, yellow, green, blue and violet contours. The portion of the red color is the lowest energy ions (0–0.1 keV) concentrated at the center, which is similar to the distribution shown in Fig. 3 for the magnetosheath ions. Thus,

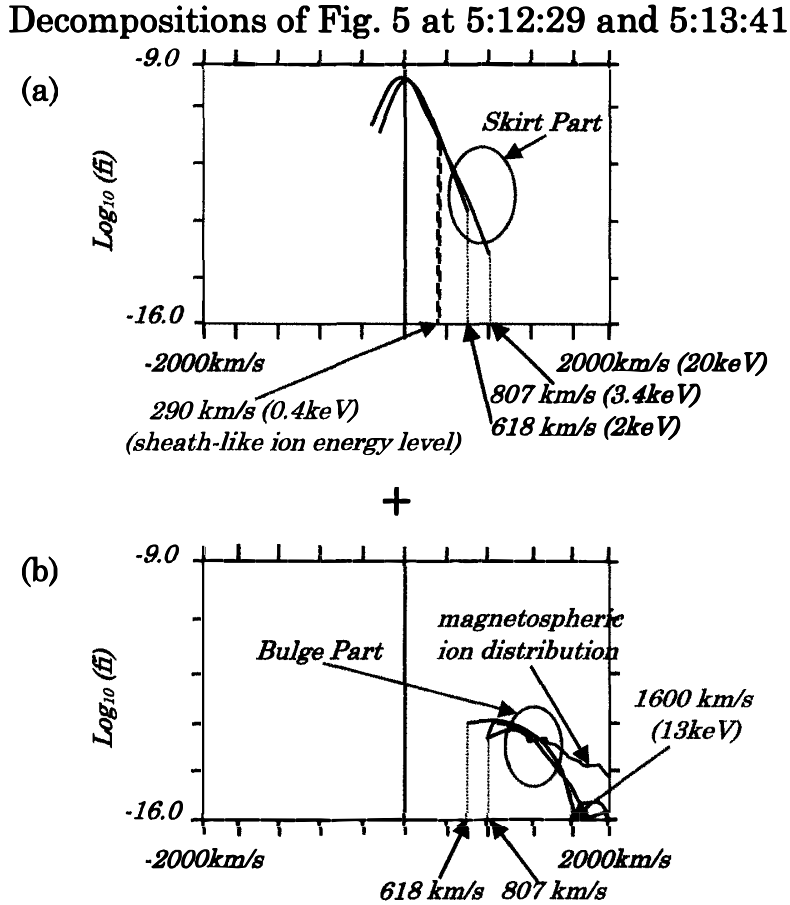

Fig. 6. The ion one dimensional distribution curve shown in Fig. 5 is decomposed into two parts. The top (a) shows the magnetosheath-like low energy ions with a monotonic slope that extends to the intermediate energy range between the magnetosheath ions and magnetospheric ions (2–3 keV). The bottom (b) shows a bulge in the energy range from 2–3 keV to13 keV, which does not extend to the magnetospheric high energy range (20 keV~). The magnetospheric high energy distribution is shown with a red curve.

this portion is a piece of evidence showing that the low energy magnetosheath ions are observed with this impulse and suggests that they penetrate into the inner magnetosphere. Next, the yellow colored portion corresponds to the energy of 0.5–1.0 keV, a little higher than the magnetosheath ions. The green color also corresponds to the energy of 1.0–3.0 keV, and remaining portions are those of blue (3.0–10 keV) and violet colors (10 keV~).

The characteristics described above are easily understood by using the one dimensional distribution function taken along the magnetic field line as shown with the red broken line, which is shown in the right panel. The distributions obtained at the first and second impulses at 0512:29 UT and 0513:41 UT are superimposed with violet and green curves. The distribution characteristics of two curves are different from the ion distribution in the magnetosphere given with the red curve obtained at 0510:17 UT for reference.

In order to understand more clearly the distribution characteristics in this panel we represent a decomposition of them into two parts shown in Fig. 6. One is the

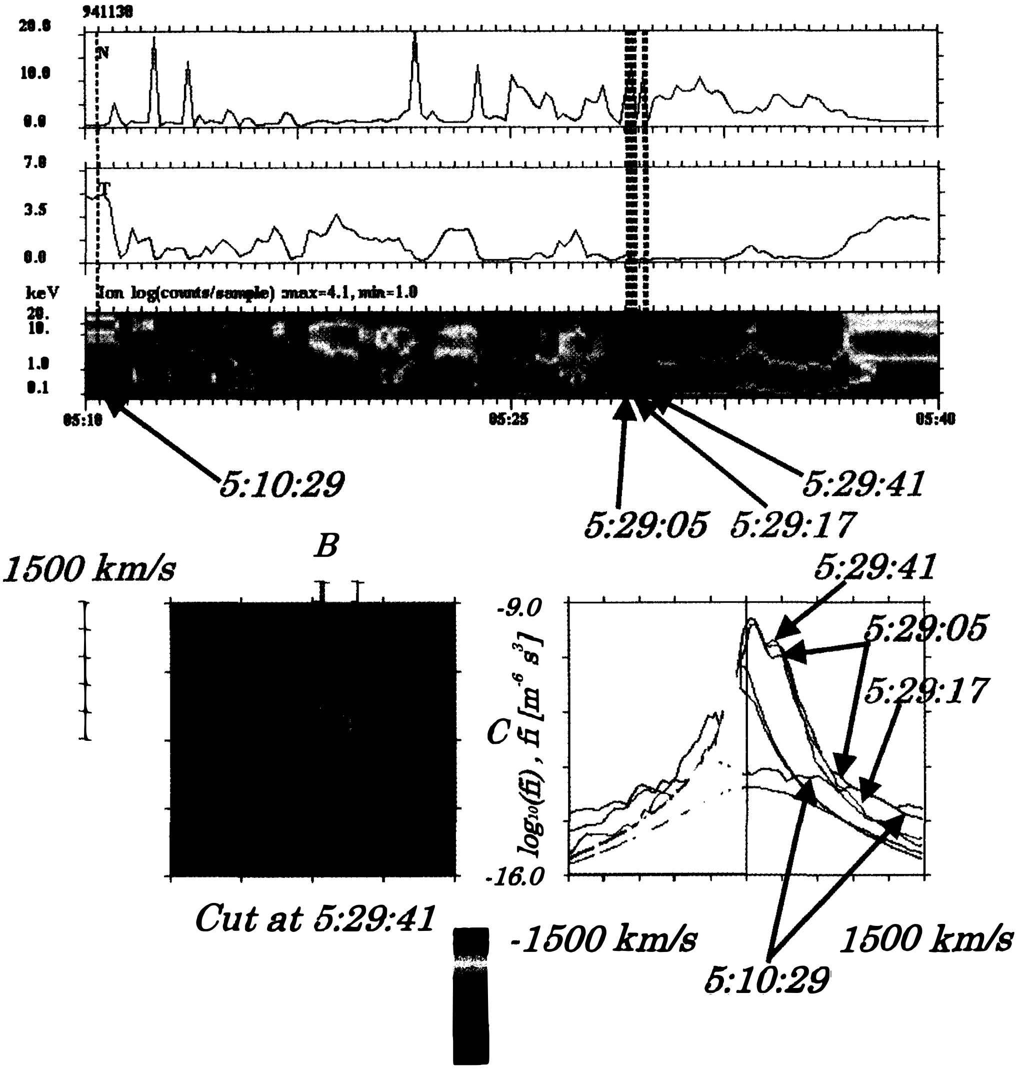

Fig. 7. Ion distribution functions of the impulses occurred during about 1 min from 0529:05 to 0529:41 UT. Format is the same as in Fig. 5. The two dimensional distribution function is distorted in its shape in perpendicular direction to the magnetic field line stronger than the case shown in Fig. 5. But the accelerated ions originated from the magnetosheath are also distributed to the field-aligned direction and one dimensional distribution function shows the coexistence of the sheath-like cold ions and their accelerated ions, which is seen as bumps and slopes in the lower right diagrams.

distribution in the low energy part (a) with a peak with monotonic slope extending to the energy 2.0–3.0 keV. The other part (b) is a bulge in the energy range covering from 3.0 keV to 13 keV, which does not extend to the high energy tail of the magnetospheric ions (20 keV).

Comparing these distributions with the typical distribution of the magnetosheath ions, the difference becomes clear. The distributions given with the violet and green lines shown in Fig. 6a have a similar skirt in contrast to a monotonic distribution without a skirt for the magnetosheath ions shown in Fig. 3. They also show a bulge in the intermediate energy range between the magnetosheath and magnetosphere (Fig. 6b). The bulge does not extend to the higher energy tail characterized as the magnetospheric

Decompositions of Fig. 6 at 5:29:05, 5:29:17 and 5:29:41

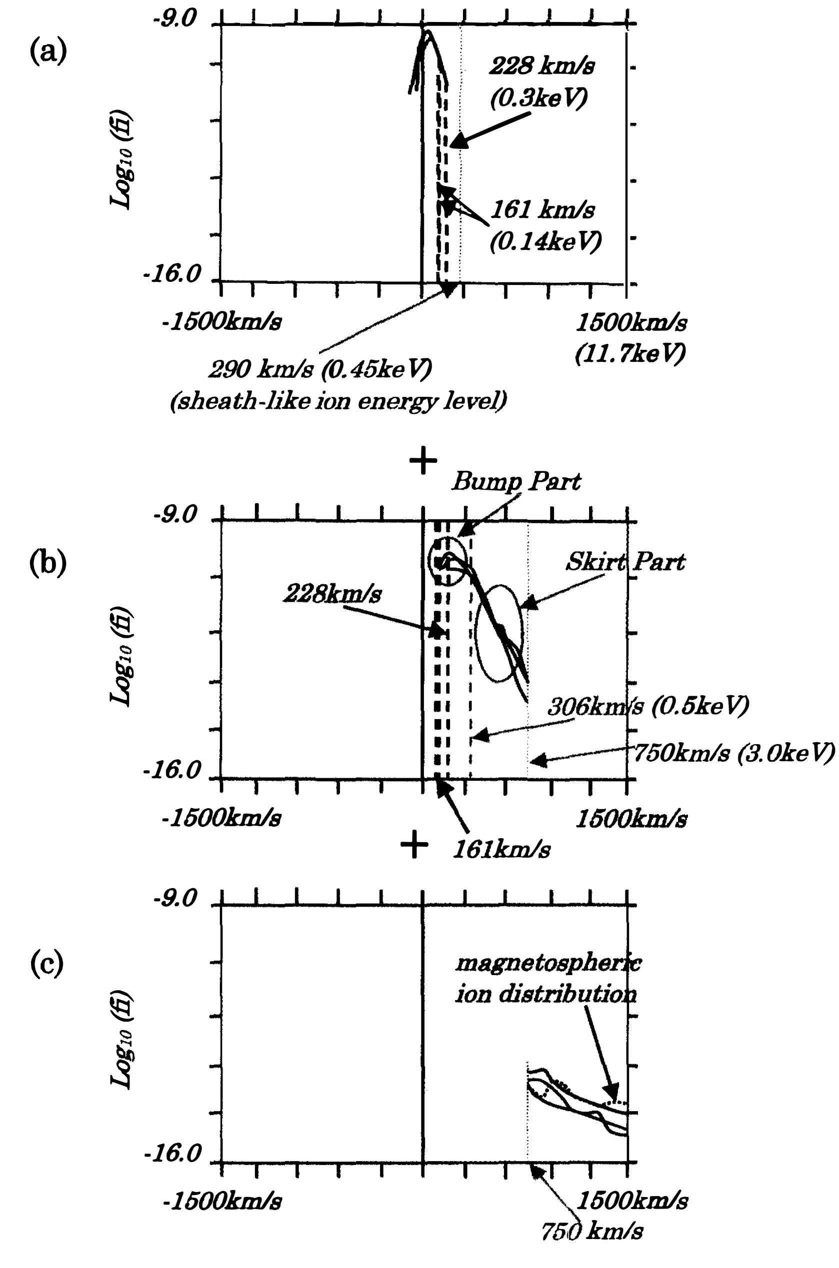

Fig. 8. The ion one dimensional distribution function shown in Fig. 7 is decomposed into three parts. Format is the same as in Fig. 6. The top (a) shows ions of the very low energy with a monotonic curve extending to the energy range of 0.14 keV and 0.3 keV. The middle (b) is a bump with a slope in the energy range from 0.3 keV to 3 keV. The bottom (c) shows the ion distribution for the energy range from 3 keV to 12 keV. The magnetospheric ion distribution is superimposed with the violet dashed line.

ions shown with the red curve.

Therefore, the distribution characteristics examined above for the both impulses are entirely different from the characteristics observed for the magnetosheath and magnetospheric ions. These results indicate that the ions that were confirmed in the impulses have a mixed characteristic between the intrinsic magnetosheath and magnetospheric ions. In addition, from this distribution, a kind of acceleration and/or broadening process for the distribution are required to explain the distribution in the intermediate energy range.

Examples for the ion distribution function of the other impulses occurred successively are illustrated in Fig. 7, which shows the distribution curves of three impulses occurred at 0529:05 UT, 0529:17 UT and 0529:41 UT. The format of Fig. 7 is the same as shown in Fig. 5. The ion phase space density profile obtained for the impulse at 0529: 41 UT is given in the bottom left panel. As seen in the previous example at 0512:29 UT, the magnetosheath ions also concentrated at the center. However, in this example the orange-colored contour appears clearly and extends to the higher energy range shown with the colors of yellow, green, blue and violet. One dimensional distribution functions for the three impulses are shown in the right panel. The details of these distributions are given in Fig. 8. This figure shows a decomposition of the distributions given in Fig. 7. It consists of three parts, (a), (b) and (c). The top figure (a) shows the distribution of the low energy part, consisting of a low energy peak with a monotonic slope that extends to 0.3 keV at most. The middle figure (b) illustrates a bump with a skirt also in the lower energy range from 0.3 keV to 3.0 keV. The bottom (c) shows the intermediate energy range (3.0 keV$\sim$).

The comparison of the distributions shown in Fig. 8 with typical distributions for the magnetosheath and magnetospheric ions given in Figs. 3 and 4 shows the following observed facts.

The part (a) corresponds to the low energy ions, which means the magnetosheath ions. The distribution shown in Fig. 8b has a bump in the lower energy, which appears at the energy of 0.3 keV and in addition, the skirt extends to the intermediate energy range between the magnetosheath and magnetospheric ions (0.5–3.0 keV). The bulge seen in Fig. 5 is not recognized in Fig. 8. The higher energy tail shown in (c) corresponds to the distribution of the magnetospheric ions shown with the violet broken line in Fig. 8. Therefore, the distributions demonstrated in Fig. 8 are revealed to consist of the three parts, *i.e.*, the sheath-like ions, magnetospheric ions and accelerated or broadened ions of the intrinsic magnetosheath ions.

Two important points are to be noticed in Fig. 8. One is a bump in the lower energy part, which was not identified in the previous examples. The other is an extent of the skirt to the intermediate energy. The bump and extended skirt in the intermediate energy range are important, because they suggest that the magnetosheath low energy ions are accelerated by the process of the impulsive magnetic field variations.

Therefore, we can conclude that the impulses examined here would be due to a certain acceleration mechanism such as a magnetic reconnection at the magnetopause.

4. Summary and Discussion

We have examined impulses of the magnetic field, plasma density and temperature, which were observed inside of the magnetopause LLBL. The characteristics associated with these impulses are summarized as follows.

1) A sudden change of the magnetic field orientation was recognized.
2) Magnetic field strength decreased.

3) On the other hand, ion density increased.
4) Ion temperature decreased.
5) Ion distribution function showed a broadening in the low energy distribution.
6) A bump and its extending skirt were confirmed at the intermediate energy range between the magnetosheath and magnetospheric ions.

The first two points seem to be related to the magnetic field signature showing the diamagnetic effect by a development of the field-aligned current. Next two points are related to the penetration of the magnetosheath-like low energy and dense plasma into the inner magnetosphere in association with the impulses. The last two points are related to the characteristic changes of the penetrated plasma on the way of the penetration. The plasma is revealed to be unlikely originated from both the magnetosheath and magnetospheric plasmas. The characteristics show that some acceleration mechanism is operating to the magnetosheath plasma such as a reconnection process at the magnetopause, leading to the impulsive variations.

NAKAMURA *et al.* (1997, 1998) gave some pieces of evidence of such a magnetic reconnection at the magnetopause. In their papers, the evidence of plasma acceleration was shown with a clear bump appeared in the distribution in the lower energy range, which is similar to the observational fact described in the present paper. The bump that was dealt with NAKAMURA *et al.* (1996) occurred sequentially, and were interpreted with a "velocity filter effect" due to the magnetic field reconnection. Thus, the bump is one of the important keys to make clearer whether the magnetic reconnection is taking place or not. Such a bump in the velocity distribution was found in our present examination. Therefore, this observed result concludes that the observed impulses are closely related to magnetic reconnection process.

Figure 9 illustrates the superimposition of the one dimensional ion velocity distribution functions observed in the impulses shown in Figs. 5 and 7 and typical distributions of both the magnetosheath and magnetospheric ions shown in Figs. 3 and 4. The green and violet broken curves show the distribution in the impulse observed at 0512:29 UT and 0529:05 UT, respectively. The blue and red curves show typical distribution of the magnetosheath and magnetosphere ions. Comparing these distributions, the ion distribution observed in the impulse variations of the magnetic field and plasma has a bump

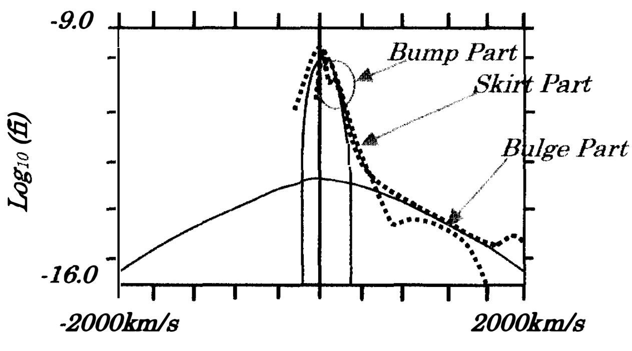

Fig. 9. The one dimensional ion velocity distribution functions shown in Figs. 3, 4, 5 and 7 are superimposed. Format is the same as in the previous figures. The blue curve shows a typical magnetosheath ion velocity distribution. The red curve shows typical plateau-like magnetospheric one. The green- and violet-dotted curves show the velocity distribution function observed at 0512:29 UT and 0529:05 UT, respectively.

part in low energy region (0–0.4 keV). The extent of the distribution skirt caused by the acceleration for the low energy ions and a bulge are found in intermediate energy range (0.5–3.0 keV). The extent and a bulge cannot be identified in the distributions of both the ions in the magnetosheath and magnetosphere. In the impulse observed at 0529:05 UT, a part of the ion distribution is superimposed on the typical magnetospheric ion distribution. Above observational facts mean that the ion distributions in the impulses are different in each impulse variation and do not contain a simple mixture of both magnetosheath and magnetospheric ions. Therefore, the plasma appeared in the impulses are considered to be accelerated. As this result, the velocity distribution was broadened to the field-aligned direction.

From Fig. 2, the beta ratios in these impulses were very high. Thus, the magnetic field strength decreased in association with the appearances of the impulses due to the diamagnetic effect of the ions. This magnetic field depression is not found in the FTEs, in which the magnetic field strength increases and associates a bi-polar shaped field in B_z component (ELPHIC *et al.*, 1995).

Therefore, we can obtain the following conclusions;

1) The important characteristics of the ion distribution functions observed in impulses are demonstrated as a bump and broadening of the distribution in low energy range and a bulge in intermediate energy range.

2) These characteristics cannot be explained only with a simple mixing process of both ions in the magnetosheath and magnetosphere.

3) Therefore, a kind of acceleration and/or heating mechanism to the magnetosheath ions is necessary.

Acknowledgments

We would like to express our sincere thanks to all members of the GEOTAIL project team, and also grateful to M. NAKAMURA, Earth and Planetary Science, Tokyo University for his useful discussions and criticisms.

References

ELPHIC, R. C. (1995): Observations of Flux Transfer Events: A review. Physics of the Magnetopause, ed. by P. SONG *et al.* Washington, D.C., Am. Geophys. Union, 455–471 (Geophys. Monogr. Ser., **90**).

GOSLING, J. T., THOMSEN, M. F., BAME, S. J. and ONSAGER, T. G. (1990a): The electron edge of the low latitude boundary layer during accelerated flow events. Geophys. Res. Lett., **17**, 1833–1836.

GOSLING, J. T., THOMSEN, M. F., BAME, S. J., ELPHIC, R. C. and RUSSELL, C. T. (1990b): Plasma flow reversals at the dayside magnetopause and the origin of asymmetric polar cap convection. J. Geophys. Res., **95**, 8073–8084.

NAKAMURA, M., TERASAWA, T., KAWANO, H., FUJIMOTO, M., HIRAHARA, M., MUKAI, T., MACHIDA, S., SAITO, Y., KOKUBUN, S., YAMAMOTO, T. and TSURUDA, K. (1996): Leakage ions from the LLBL to MSBL: Confirmation of reconnection events at the dayside magnetopause. J. Geomagn. Geoelectr., **48**, 65–70.

NAKAMURA, M., FUJIMOTO, M., KAWANO, H., MUKAI, T., SAITO, Y., YAMAMOTO, T., TSURUDA, K., TERASAWA, T. and KOKUBUN, S. (1997): GEOTAIL observation at the dayside magnetopause -Confirmation of reconnection events-. Adv. Space. Res., **17** (in press).

NAKAMURA, M., SEKI, K., KAWANO, H., OBARA, T. and MUKAI, T. (1998): Reconnection event at the dayside magnetopause on January 10, 1997. Geophys. Res. Lett., **25**, 2529–2532.

PASCHMANN, G., HAERENDEL, G., PAPAMASTORAKIS, I., SCKOPKE, N., BAME, S. J., GOSLING, J. T. and RUSSELL, C. T. (1982): Plasma and magnetic field characteristics of magnetic flux transfer events. J. Geophys. Res., **87**, 2159–2168.

RUSSELL, C. T. and ELPHIC, R. C. (1978): Initial ISEE Magnetometer results: Magnetopause observations. Space Sci. Rev., **22**, 681–715.

SCKOPKE, N. (1991): Plasma structure near the low-latitude boundary layer: A rebuttal. J. Geophys. Res., **96**, 9815–9820.

SCKOPKE, N., PASCHMANN, G., HAERENDEL, G., SONNERUP, B.U.Ö., BAME, S. J., FORBES, S. J., HONES, E. W., Jr. and RUSSELL, C. T. (1981): Structure of the low-latitude boundary layer. J. Geophys. Res., **86**, 2099–2110.

THOMSEN, M. F., STANSBERRY, J. A., BAME, S. J., FUSELIER, S. A. and GOSLING, J. T. (1987): Ion and electron velocity distributions within flux transfer events. J. Geophys. Res., **92**, 12127–12136.

(Received November 27, 1997; Revised manuscript accepted May 20, 1998)